Ceramics International 43 (2017) 12408–12419

Contents lists available at ScienceDirect

Ceramics International

journal homepage: www.elsevier.com/locate/ceramint

Apply ^{29}Si, ^{27}Al MAS NMR and selective dissolution in identifying the reaction degree of alkali activated slag-fly ash composites

X. Gao[a,b], Q.L. Yu[b,*], H.J.H. Brouwers[a,b]

[a] State Key Laboratory of Silicate Materials for Architectures, Wuhan University of Technology, Wuhan 430070, PR China
[b] Department of the Built Environment, Eindhoven University of Technology, P.O. Box 513, 5600 MB Eindhoven, The Netherlands

ARTICLE INFO

Keywords:
Reaction degree
Alkali activation
Slag-fly ash blends
Selective dissolution
^{29}Si MAS NMR
^{27}Al MAS NMR

ABSTRACT

This paper characterizes the phase composition and reaction degree of alkali activated slag, fly ash and their blends by using ^{29}Si, ^{27}Al MAS NMR and selective dissolution; with special emphasis on the effect of activator modulus and the usage of blended binders. The results revealed that in alkali activated slag systems, the increase of the activator modulus leads to a reduction of slag reactivity, together with significantly increased Q3(1Al) and reduced Q2(1Al) groups. Selective dissolution contributes to distinguish the unreacted fly ash and reaction products; ^{29}Si, ^{27}Al MAS NMR analyses were carried out on both components and their compositions were quantified in detail. Both polymerized Q4 structures and Q3 to Q0 sites were formed, and increasing the activator modulus resulted in an increased content of Q4 groups. When a blended system was applied, the slag reactivity was reduced with the increased fly ash reaction degree, the blended binder exhibited higher contents of newly formed Q4 groups with reduced Si/Al, reduced Q0 sites, shifted mean chain length and Si/Al of the formed C-A-S-H type gels, indicating gel interaction. Applying these two testing methods together brings new insights in understanding the structural composition of alkali activated slag, fly ash and their composites.

1. Introduction

Alkali activated materials (AAMs) have been widely investigated in recent years due to their excellent performances together with lower environmental impacts compared to ordinary Portland cement (OPC) [1–6], exhibiting the potential to be applied as sustainable alternative binders. Based on their composition, AAMs can be classified into two types: calcium enriched (Ca + Si) system and aluminosilicates dominated (Si + Al) systems [7]. The high calcium systems usually result in a reaction product of tobermorite-like C-A-S-H gel with a low Ca/Si ratio and a high Al content [8], while the major product for Si + Al systems is a three-dimensional N-A-S-H type gel [9]. Research interests are also paid to the blended alkali systems that are prepared by mixing high calcium contained raw materials with low calcium aluminosilicates, due to several modified properties regarding setting times, workability, shrinkage, mechanical properties and durability compared to the individual ones [10–13]. The structure of the reaction products is mainly depending on the activator type and dosage, raw materials composition and curing conditions, but can be generally regarded as coexisting calcium silicate hydrate (C-A-S-H) and aluminosilicates hydrate (N-A-S-H) type gels [14–16]. The reaction includes complex chemical and thermodynamic processes and the large amount of available calcium and aluminate affect the original structure of N-A-S-H and C-(A)-S-H gels, respectively [17–19].

Various types of analyzing methods are applied in order to understand the chemistry, reaction process and products of this new binder system by using isothermal calorimetry, Thermo-gravimetric and Differential Scanning Calorimeter (TG/DSC), Fourier Transform Infrared Spectroscopy (FTIR), X-ray Diffraction (XRD) and Scanning Electron Microscopy with an energy dispersive spectrometer (SEM/EDX). Together with those testing methods or working on its own, Magic Angle Spinning (MAS) Nuclear Magnetic Resonance (NMR) spectroscopy presents new insights in phase evolution of the reaction products. For instance, in the alkali activated high calcium systems, blast-furnace slag is the mostly widely studied material. The presence of 4–6 coordinated Al environments and their chemical shifts during the reaction were identified by ^{27}Al MAS NMR, as well as the Al substitution in C-S-H gels as bridging tetrahedral and AFm, hydrotalcite-like phases from octahedral Al (not always XRD identifiable) were observed [20–25]. ^{29}Si MAS NMR resonances show the presence of Q0 monomers, Q1 dimers and Q2 bridging groups [8,20,26–30]. As for the alkali activated aluminosilicates, commonly investigated precursors are fly ash and metakaolin. The ^{29}Si MAS NMR spectra reveal that the silicates usually present in Q4(mAl) structures, and their

* Corresponding author.
E-mail address: q.yu@bwk.tue.nl (Q.L. Yu).

http://dx.doi.org/10.1016/j.ceramint.2017.06.108
Received 18 March 2017; Received in revised form 17 May 2017; Accepted 18 June 2017
Available online 20 June 2017

compositions are depending on the key synthesizing factors such as activator compositions and curing conditions [31–35]. Moreover, the deconvolution of the obtained spectra makes quantitative analysis possible, especially on the ^{29}Si NMR, which provides further information about the structure changes, chain lengths, elements' ratios (mainly Ca/Si and Si/Al) of the reaction products. This method has gradually become an accepted approach to provide a qualitative investigation based on the quantified results [20,36–43].

Attentions have also been paid to using NMR to investigate more complex blended alkali systems, containing both high calcium and aluminosilicate phases (N-A-S-H + C-A-S-H). The existence of Q0 to Q2 and Q4 silicon units determined by ^{29}Si NMR verifies the presence of two different types of reaction products in the blended system [30,45], while the gel interaction was observed by using ^{29}Si and ^{27}Al MAS NMR together with XRD, SEM/EDX and TEM/EDX. By tracking the structural shifts of Si and Al, it is observed that the mixture of C-S-H and N-A-S-H gels at initial stage is affected by the dissolved Ca and Al groups and gradually their composition are changed into C-A-S-H and N-C-A-S-H gels, respectively [44]. ^{29}Si MAS NMR with peak deconvolutions was also used to analyze the reactivity of the starting materials indirectly by quantifying the phase changes in the blended system, for instance the indirect quantitative analysis to study the effect of slag to fly ash ratios and activator type on reactivity [39], quantifying the influence of carbonation on alkali activated slag and slag-fly ash blends by ^{29}Si NMR [20], evaluating the phase composition of a chemically synthesized N-A-S-H/C-A-S-H mixture by TG, FTIR together with ^{29}Si NMR [37], characterizing the phase composition, chain length, Si/Al ratios and reaction degree of hydroxide activated slag-metakaolin blends by applying ^{29}Si and ^{27}Al NMR [46].

Although great achievements have been made based on MAS NMR analysis, there are still remaining issues that deserve further discussions in blended alkali systems. One problem lays in the ^{29}Si NMR spectra of aluminosilicates, especially for the fly ash, both the solid precursor and reaction products show overlapped resonances that usually range from around −70 to −120 ppm, assigning to the Q4(mAl) units [20,39,40]; those overlapped peaks make it difficult to track their origins, therefore the quantitative analysis can only provide qualitative conclusions on the structural changes and it is impossible to identify the reactivity. However, previous studies proved a feasible manner to separate the unreacted fly ash from the reacted aluminosilicates by HCl treatment [34,47,48], thus theoretically it is possible to quantify the reaction degree and Si structure shifts by comparing the ^{29}Si NMR results of samples before and after HCl treatment. Another issue is the commonly used silicate based activator; those additional silicates participate into the reaction process and become part of the reacted gels, and the activator dosage and modulus also strongly affect the silicate structure and reaction chemistry [33], while those findings are rarely linked to the reaction degree of blended alkali systems. Furthermore, alkali activated aluminosilicates are usually investigated in high alkali conditions with elevated temperatures to pursuit ideal mechanical properties, while in the blended systems, relatively low alkalinities and temperatures are more commonly used due to the calcium enriched precursors; how those starting conditions affect the original Si + Al systems need to be further clarified.

The aim of this study is to carry out a quantitative investigation on the reaction degree of ambient temperature cured silicate activated slag, fly ash and their blends based on the ^{29}Si and ^{27}Al MAS NMR spectroscopy, with special emphasis on the influence of precursors' interaction and activator modulus. The phase compositions are evaluated by deconvoluting the NMR peaks, and the reaction products are selectively dissolved in order to extract the unreacted phases. The effects of precursors and activators on reaction degree are discussed in detail, and subsequently conclusions are drawn based on the quantified NMR investigations.

Table 1
Major chemical compositions of the starting precursors.

Oxides (wt%)	FA	GGBS
SiO_2	54.62	34.44
Al_2O_3	24.42	13.31
CaO	4.44	37.42
MgO	1.43	9.89
Fe_2O_3	7.21	0.47
Na_2O	0.73	0.34
K_2O	1.75	0.47
SO_3	0.46	1.23
LOI	2.80	1.65

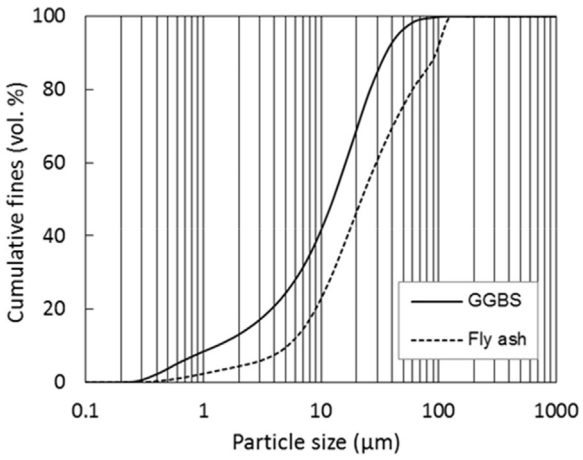

Fig. 1. Particle size distributions of the raw materials.

2. Experiment

2.1. Materials

The solid precursors used in this study are commercially available ground granulated blast furnace slag and Class F fly ash. Their major chemical compositions and particle size distributions are shown in Table 1 and Fig. 1, respectively. The X-ray diffraction patterns of the used slag and fly ash are shown in Fig. 2. The slag shows a peak hump between 25 and 35° due to the amorphous components and no significant crystalline phases were observed; while the fly ash has an amorphous hump between 15 and 30° and contains crystalline phases such as quartz (SiO_2), mullite ($Al_6Si_2O_{13}$), maghemite and hematite (Fe_2O_3); while the slag exhibits mostly amorphous phases. In terms of the alkaline activators, a mixture of sodium hydroxide (pellets, 99 wt%)

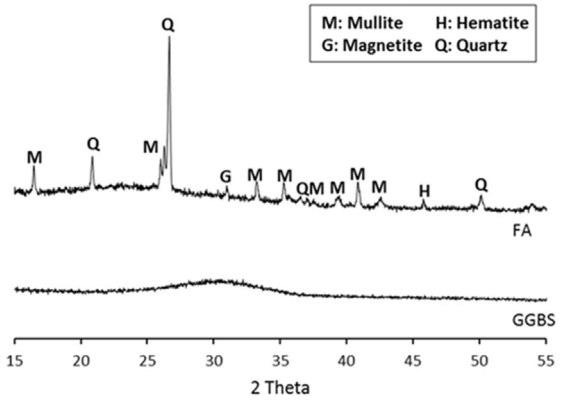

Fig. 2. The X-ray diffraction patterns of the starting materials.

and a commercial sodium silicate solution (27.69% SiO_2, 8.39% Na_2O and 63.92% H_2O by mass) was used. The desired activator modulus (Ms, i.e. SiO_2/Na_2O molar ratio) was achieved by adding the appropriate amount of sodium hydroxide into the sodium silicate solution. Distilled water was added in order to reach the desired water/binder ratio. The mixed activator solution was cooled down to room temperature for 24 h before further use.

2.2. Experiments

The alkali activators used in this study had a constant equivalent sodium oxide (Na_2O) content of 5% by mass of the binder and activator modulus of 0.8, 1.6 and 2.4, respectively. The target activator modulus was reached by mixing sodium silicate solution and sodium hydroxide pellets with suitable ratios. The water/binder ratio was kept constant at 0.35 in all mixtures. The water consisted of the added distilled water and the water contained in the activator solution. Three binder compositions were used: pure slag, pure fly ash and slag-fly ash blends (50/50 by mass). All specimens were cured at room temperature and a relative humidity of 95% for 1 month.

Solid-state MAS NMR spectra were acquired using a Bruker Avance 400WB spectrometer. The ^{29}Si NMR spectra were collected at 79.5 MHz on a 7 mm probe, with a pulse width of 6.5 μs, a spinning speed of 15.9 kHz and a relaxation delay of 10 s. The ^{27}Al MAS NMR spectra were obtained by using a 4 mm probe, at 104.5 MHz with a pulse width of 6.5 μs, a spinning speed of 41.7 kHz and a recycle delay of 2 s.

The selective dissolution method for analyzing alkali activated fly ash and slag-fly ash blends was applied following the description of Fernandez et al. [34] and Puligilla et al. [47], respectively. Samples were firstly ground and then dissolved in 1:20 HCl (vol%). Specifically, 1 g of reacted powder was added into 250 ml of HCl solutions, the mixture was then stirred for 3 h and filtered by using a 2 μm filter paper. The insoluble residues were washed with distilled water until a neutral pH is reached, then dried and stored until the analysis was carried out. Selective dissolutions were repeated 3 times for each mix. The acid attack decomposes the original structure of slag and its reaction products, as well as the N-A-S-H type gels or other reacted phases, leaving behind the unreacted fly ash as the only insoluble residue.

3. Results and discussion

3.1. Characterization of precursors and activators

The ^{29}Si MAS NMR spectra of the two starting materials, slag and fly ash, are presented in Fig. 3(a) and (b). The unreacted slag shows a broad peak that ranges from −55 to −95 ppm, centered at around −75 ppm. This broad shaped peak can be generally regarded as the amorphous Q0 or Q0+Q1 sites within the glassy structure. During this study, the Q sites from the anhydrous slag are considered as one single phase, also its curve shape after alkali activation is assumed to be unchanged [37,46]. In the later deconvolution investigations, its spectrum range is fixed and the intensity is rescaled to evaluate the contribution of the raw slag in the reaction products. The spectrum of the initial fly ash presents a broad overlapped peak within the range of −80 and −120 ppm, this poorly defined area suggests the heterogeneous presence of different Q4 structures. The deconvolution of the overlapped peaks in fly ash was carried out in Origin Pro 9.0 by applying the Gaussian line model, nine Q4 sites were identified, and constant peak widths and locations are used throughout the whole study. The peaks at −86, −90, −94, −98, −101, −104, −108, −112, −116 ppm are assigned to the Q4(mAl, m = 0–4) groups; both the starting vitreous components and crystalline phases like quartz and mullite show a contribution to those sites [33,49,50].

Fig. 3(c) shows the ^{27}Al MAS NMR spectra of the initial slag and fly ash. The Al environments in those two materials are usually identified in three types: the tetrahedral Al that ranges from approximately 50 to 100 ppm, the pentahedral Al that usually shows between 30 and 40 ppm, and the octahedral region (−10–20 ppm). The original slag presents a broad resonance between 0 and 80 ppm and centered at around 55 ppm, indicating a combination of Al(IV), Al(V) and Al(VI) sites [49,51] instead of a well-defined single Al environment. This can be attributed to the structure of glassy phases in the original slag. In terms of the initial fly ash, a broad peak at around 46 ppm assigned to the tetrahedral Al is identified, as well as a narrow octahedral Al peak around 2 ppm. It has been reported that the resonance at around 2 ppm is attributed to the Al components from mullite.

The ^{29}Si NMR spectra of the activator solutions are presented in Fig. 4. The activator with a modulus of 0.8 shows an evident peak at around −72 ppm, indicating the presence of Q0 monomers. Besides, Q1 and Q2 groups with relatively low peak intensities can be observed, as well as limited amount Q3 sites that are located at around −98 to −100 ppm. Increasing the activator modulus results in a significant increase of Q groups with a higher polymerization degree, as can be seen that shifting the activator modulus to 1.6 and then 2.4, the intensity of peaks for Q1 dimers becomes more evident, indicating the increasing fraction of those units within the activator solution. Also, peaks for Q2 and Q3 units are obviously showing a higher intensity with larger covered area, especially for Q3 groups that are located at around −95 to −100 ppm. It should be noticed that no significant peaks are found lower than −100 ppm in all cases, which suggests that no Q4 sites are present in the activator. It is already known that the different Q compositions of the activator is a combined result of the pH and silicate dosage, and less polymerized Q groups would present a higher reactivity during the alkali activation [59]. The effect of activator modulus on reaction degree and the structure of the reaction products will be analyzed by solid state MAS NMR after the mixtures are reacted and hardened.

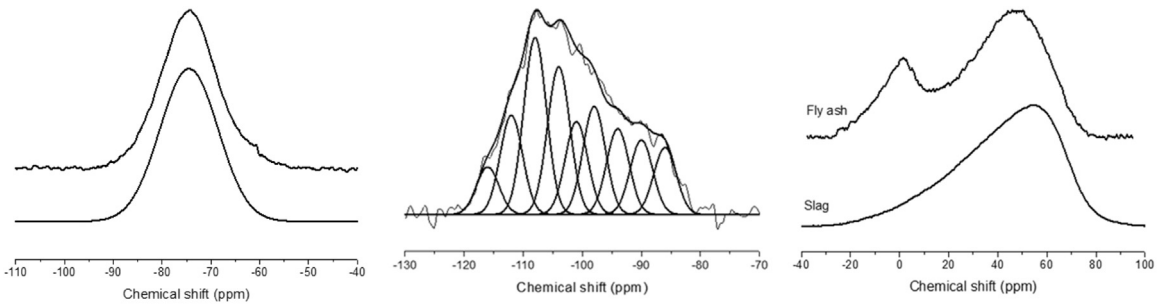

Fig. 3. The NMR spectra of raw materials (a: ^{29}Si NMR of slag, b: ^{29}Si NMR of fly ash, c: ^{27}Al NMR of slag and fly ash).

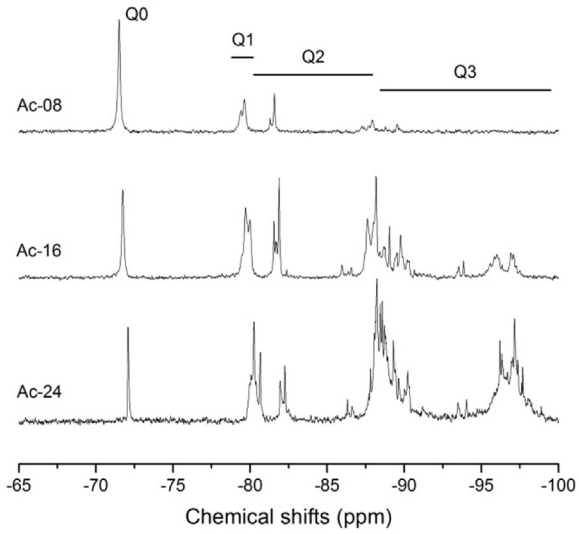

Fig. 4. The ^{29}Si MAS NMR spectra of the activators.

3.2. Alkali activated slag

3.2.1. ^{29}Si MAS NMR

Fig. 5(a)–(c) show the ^{29}Si MAS NMR spectra of alkali activated slag with activator modulus of 0.8, 1.6 and 2.4, respectively. The obtained spectrum, fitted peak and the deconvoluted results are presented. For mixes with the lowest activator modulus (i.e. Ms of 0.8), eight deconvoluted peaks are presented. The broad one from around −55 to −95 ppm refers to the unreacted slag. Its reactivity can be calculated indirectly by comparing its total content before and after reaction. The peak located at around −75.2 ppm refers to the Q0 sites, suggesting the presence of isolated silica tetrahedral within the reaction products. Due to the fact that a single Q1 group cannot perform an ideal peak fitting, two Q1 peaks representing the non-bridging structure are separated: Q1-a and Q1-b that are located at about −76.8 and −79.0 ppm, respectively. It is commonly agreed that this site mainly refers to the end of chain silicate tetrahedrals within the newly formed C-(A)-S-H type gels [37]. Previous studies also observed two Q1 sites within the reaction products of alkali activated slag and its blends, while their differences in the chemical environment are not discussed in detail [20,52,53]. Three types of Q2 groups are observed in the reaction products: Q2(1Al) sites located at around −81.6 ppm, Q2-b and Q2-p sites at approximately −84.2 and −85.7 ppm, respectively. Those Q2 sites are assigned to the middle-of-chain silicates with either bridging or pairing conditions within the C-(A)-S-H gels [43,58]. In addition, there is a small amount of high crosslinking Q3(1Al) sites (around −89 ppm) that is in line with previous studies [25,53,55].

Table 2
Deconvolution results of ^{29}Si MAS NMR spectra of alkali-activated slag.

Chemical shift (± 0.5 ppm)	Site type	Sample ID		
		AS-08	AS-16	AS-24
−74.51	Qs	30.28	32.27	41.09
−74.5	Q0	7.38	9.39	7.09
−76.9	Q1-a	4.03	5.31	5.00
−78.7	Q1-b	14.85	11.07	8.09
−81.5	Q2(1Al)	28.26	16.27	10.69
−84.4	Q2-b	10.24	12.44	9.75
−86.5	Q2-p	2.16	3.87	5.65
−89.2	Q3(1Al)	2.81	9.38	12.63

As the activator modulus increases to 1.4 and then 1.8, there is an obvious increase of the covering area that refers to the original slag; indicating less starting precursor has reacted. This result is in accordance with the previous investigations on the reaction kinetics and gel structures that a higher activator modulus leads to a delayed early age reaction with reduced reaction intensity, also the chemically bond water content exhibits a slight reduction [60]. Other obvious changes caused by the increased activator are the reduced relative content of Al substituted Q2 groups and the increased Q3(1Al) groups. The effect of activator modulus on the silicate structure compositions is quantified based on the deconvolution and the results are summarized in Table 2. It can be seen that the unreacted slag content in the reaction products is around 30.3%, 32.3% and 41.1% in mixtures with activator modulus of 0.8, 1.6 and 2.4, respectively. Considering the alkali solution also contributes to the total silica content, the reaction degree of slag (RD(s), in terms of Si) is calculated as follows (in mol.%):

$$RD(s) = \frac{Si(Or) - Si(Un)}{Si(Or)} \times 100\% \quad (1)$$

Where Si(Or) is the input Si from the original slag, and Si(Un) is the unreacted Si in slag with the reaction products.

The result shows that when increasing the activator modulus from 0.8 to 1.6 and then 2.4, the reactivity of Si from slag decreases from 66.3% to 60.5% and 45.1%, respectively. It indicates that although additional silicate from the activator benefits the reaction in various aspects, its dosage should be limited to a reasonable level, otherwise a negative effect in terms of the slag efficiency may take place, as well as porosity and strength [57,58], especially in the case of mixes with a high modulus of 2.4. It is suggested that the reduced pH due to the increased modulus and the increased available reactive silica at the initial age are the two reasons that lead to the reduced slag reactivity. Besides, Q1 groups (including Q1-a and Q1-b) show a gradual reduction when increasing the activator modulus. In terms of the Q2 groups, mixes with activator modulus of 0.8 and 1.6 exhibit similar content: 40.7% and 39.8%, respectively. When the modulus increases

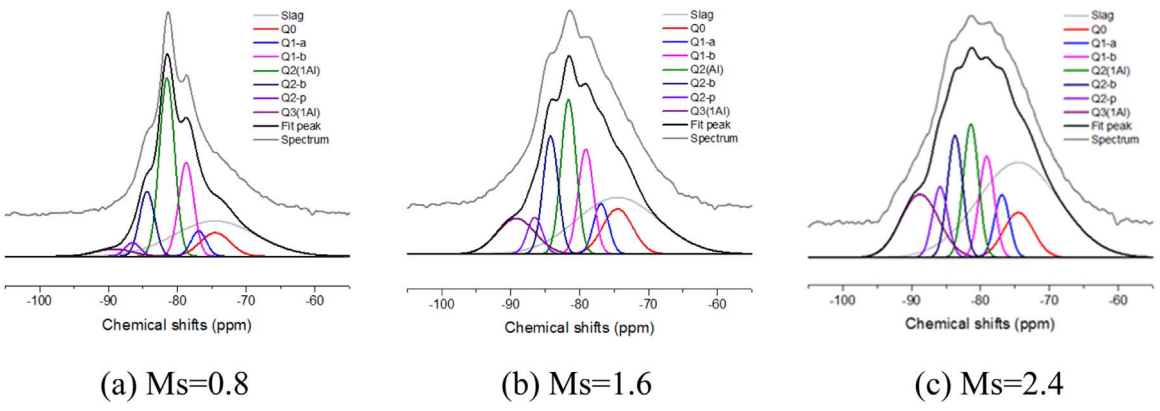

Fig. 5. The ^{29}Si MAS NMR spectra of alkali activated slag.

to 2.4, the Q2 content significantly reduces to 26.1%. It is highly possible that the shifts of Q1 and Q2 contents are related to the reaction degree of slag, since the terminal Q1 and bridging Q2 groups are the representative structures of the reaction products, and those parameters share a similar shifting tendency. Among the different types of Q2 sites, the Q2(1Al) groups present a significant reduction from 28.3% to 10.7%, due to the fact that the original slag is the only aluminate source in this case, the decreased amount of reacted slag leads to a reduction of Al supply in the solution, and therefore less Al is bonded into the C-(A)-S-H type gels. One dramatic increase as a result of the increased activator is the content of Q3(1Al) sites, from about 2.8–12.5%. It is suggested that the silicate structure in the activator solution plays an important role, since the Qn(0–4) groups are sensitive to the pH and Si/Na ratios in the solution. One previous investigation on the effect of activator parameters on silicate structures also showed that when activator modulus is around 1.0, the silicate is mainly shown in the form of Q0 to Q2 sites; when increasing the modulus to 1.7 or higher, the Q0 to Q2 sites content shows a sharp reduction while Q3 groups become more significant [59]. Criado et al. [33] observed a similar tendency regarding the effect of SiO_2/Na_2O ratios on the silicate structures on alkali solution.

3.2.2. ^{27}Al MAS NMR

Compared to the original slag, the reaction products show two significant Al peaks. As shown in Fig. 6, a significant and relatively broad peak is shown at around 62–72 ppm, which is assigned to the tetrahedral Al(IV) that is incorporated in the C-A-S-H gels with bridging conditions [60,61]; the other one with lower intensity and sharper shape at around 10 ppm is usually regarded as octahedral coordinated Al in AFm and/or hydrotalcite typed phases [62]. These phases are usually poorly crystallined in the case of alkali activated system and therefore not always XRD detectable [57,63]. Besides, the unreacted slag also contributes to the 4, 5 and 6 coordinated Al regions in the spectrum, since certain amount of raw slag is clearly identified by ^{29}Si MAS NMR. It is generally believed that the deconvolution of ^{27}Al MAS NMR peaks are more suitable for qualitative evaluation rather than quantitative calculation, due to their broad peak locations, asymmetrical natural and complicated linking environments [40,62]. Therefore the deconvolution of Al spectra was not carried out in this study.

For mixes with an activator modulus of 0.8, the tetra-coordinated region seems to exhibit two resonances: a narrow one at around 71.5 ppm and a smooth one at around 65 ppm. The presence of more than one Al(IV) site within the reaction products of alkali activated materials is also observed in previous studies, and they are all identified as the tetrahedral Al in the C-A-S-H type gels [40,41,54]. As the activator modulus increases to 1.6 and 2.4, the peak location of

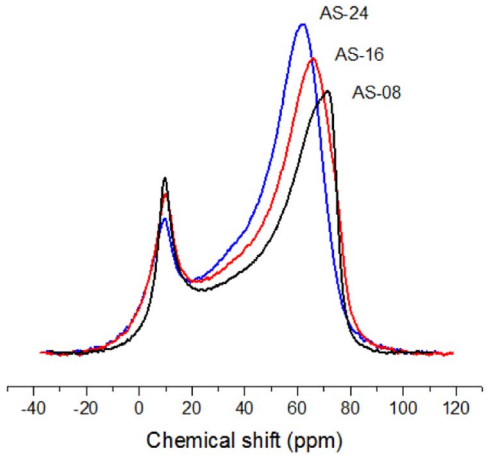

Fig. 6. The ^{27}Al MAS NMR spectra of alkali activated slag.

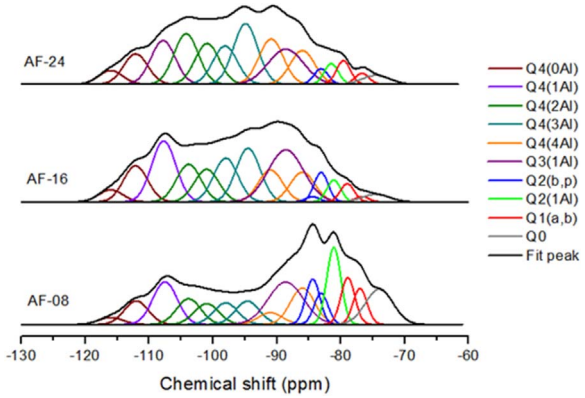

Fig. 7. The ^{29}Si MAS NMR spectra of alkali activated fly ash.

Al(IV) sites shifts to around 64 and 62 ppm, respectively; representing that slight changes occurred concerning the bonding environment surrounding the Al groups. The shifting of Al(IV) resonance into a lower chemical shift suggests a relatively high content of silicate is surrounded other than oxhydryl, therefore leading to a reduced electron density and lower ppm. This result is also in line with the ^{29}Si MAS NMR analysis that when increasing the activator modulus, less Q2(Al) and more Q3(1Al) groups are shown in the reaction products. Although the ^{27}Al MAS NMR resonances are not quantified in this case, it is still obvious that there is a decrease in the intensity of octahedral Al peaks compared to the tetrahedral ones. The reduced octa-Al intensity in the reaction products indicates that within the reacted phases, more Al is participated into the C-A-S-H gels rather than forming individual Al-riched phases. This can be explained by the Al uptake of C-A-S-H gels increases to some extent due to the increased total silicate input, which is in constant with [44,64,65].

3.3. Alkali activated fly ash

3.3.1. ^{29}Si MAS NMR

Fig. 7 depicts the ^{29}Si MAS NMR spectra of ambient temperature activated fly ash. By using different activator moduli, significant structural differences are resulted. The deconvolution results indicate that all mixes are having considerable contents of Q4 groups, including both unreacted Q4 sites from the original slag and newly formed ones. Depending on the activator modulus, all mixtures also contain certain amounts of poorly polymerized Q2 to Q0 groups. It is commonly known that in order to achieve an ideal reaction degree, the activation of fly ash is usually carried out under elevated temperature and high alkali concentrations, resulting in mainly highly polymerized N-A-S-H type gels with Q4 structures [4,5,34,66]. Thus a great structural variation can be seen in the activation of aluminosilicates when room temperature with moderate alkalinity is applied. Previous studies also observed the presence of Q2 to Q0 sites in room temperature cured fly ash [31,67].

The deconvolution calculation of the effect of activator modulus on silicate structure of alkali activated fly ash is summarized in Table 3. Mixes with an activator modulus of 0.8 exhibit an obvious difference compared to the mixes with higher modulus. The total covered area of Q2 to Q0 groups in this mix is around 39.1%, while this value is only 11.7% and 11.1% for mixtures with activator modulus of 1.6 and 2.4, respectively. As a consequence, the Q4 groups show a significantly lower value of 47.4% compared to 72.1% and 77.8% of the remaining two mixtures. It indicates that when the activator modulus is low to a certain degree, namely high pH and low additional silicate environment, a less polymerized structure is preferred under ambient temperature curing. For the isolated Q0 groups, mixtures with activator modulus of 1.6 and 2.4 show a similar content of 1.9% and 2.2%, the total contents of end-of-chain Q1 groups and Q2(1Al) sites also remain

Table 3
Deconvolution results of ^{29}Si MAS NMR spectra of alkali-activated fly ash.

Chemical shift (± 0.5 ppm)	Site type	Sample ID		
		AF-08	AF-16	AF-24
−116.0	Q4(0Al)	1.57	2.59	2.99
−112.0	Q4(0Al)	5.17	7.72	6.61
−108.0	Q4(1Al)	9.42	13.02	9.52
−104.0	Q4(2Al)	5.66	8.05	10.99
−101.0	Q4(2Al)	4.66	7.00	8.88
−98.0	Q4(3Al)	4.77	9.12	8.35
−94.0	Q4(3Al)	5.43	11.45	13.19
−91.0	Q4(4Al)	2.63	6.83	9.87
−86.0	Q4(4Al)	8.03	6.37	7.36
−88.6	Q3(1Al)	13.56	16.13	11.09
−84.4	Q2-p	5.79	0.64	0.00
−83.1	Q2-b	3.97	3.64	1.95
−81.1	Q2(1Al)	9.88	2.68	2.63
−79.8	Q1-b	5.96	2.26	2.97
−77.0	Q1-a	4.60	0.66	1.38
−74.0	Q0	8.89	1.86	2.22

at a similar level, while the content of Q2 structures shows a decrease from around 4.3–2.0%. However, for the mixes with a modulus of 0.8, the total covered areas of each above mentioned group is approximately 2 to 4 times higher. All three mixtures also show a significant presence of Q3(1Al) groups around 11.1–16.1%, which is higher than that of alkali activated slag. Concerning the Q4(mAl) units, the peak intensity of Q4(0Al) groups (around −116 and −112 ppm) is around 10.3% and 9.6% in mixes with an activator modulus of 1.6 and 2.4, respectively. Also the percentage of Q4(1Al) remains in a similar level of 21.1% and 20.5%. Those two types of Q4 groups are generally regarded as the ones containing mainly crystalline phases with relatively low reactivity within the original fly ash [32]. However, certain amounts of glassy phases may also present in those groups and participate into the reaction process. Moreover, the silicate contaminated crystalline phases also have the potential to be reactive [34]. Compared to the Q4(0Al) and Q4(1Al) sites, Q4 structures with higher aluminate substitutes exhibit a higher intensity shifts from around 1–4% between samples with an activator modulus of 1.6 and 2.4. It thus shows that high alumina incorporated Q4 groups tend to be more reactive. Regarding the mixes with activator modulus of 0.8, the each Q4 group shows a lower content of around 3–7% compared to the other two mixtures.

In order to investigate the reaction degree of fly ash, the selective dissolution experiment was carried out, as described in Section 2.2. The dissolution results together with the calculation of reaction degree are summarized in Table 4. Each dissolution result is an average of three measurements. The reliability of this method on identifying the reaction degree was verified by Palomo et al. in [34] by using ^{29}Si MAS NMR together with Rietveld XRD. The fraction of initial fly ash in the tested samples is calculated based on the designed recipes. The results indicate that similar to alkali activated slag, as the activator modulus increases from 0.8 to 2.4, there is a significant reduction of reaction degree from 66.2% to 48.0%. It also proves again that adding additional silicate and the consequently reduced pH exhibits a negative effect on the reaction degree. In order to further understand the contribution of the unreacted phases to the overall ^{29}Si MAS NMR

Table 4
Selective dissolution results of alkali activated fly ash.

Sample ID	Weighed AA-FA	FA within weighed samples	Residual	Reaction degree
AF-08	2.00 ± 0.001	1.33 ± 0.004	0.45 ± 0.004	66.2%
AF-16	2.00 ± 0.001	1.30 ± 0.003	0.61 ± 0.001	53.3%
AF-24	2.00 ± 0.001	1.27 ± 0.004	0.66 ± 0.005	48.0%

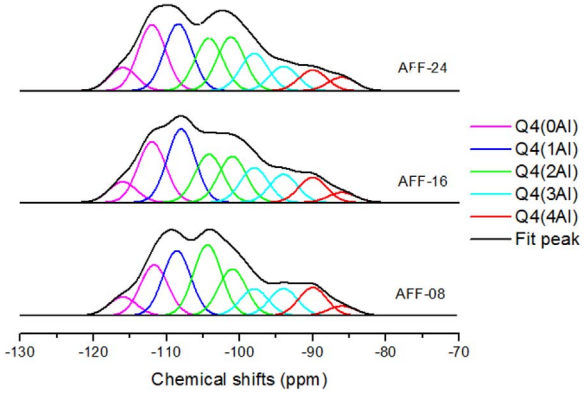

Fig. 8. The ^{29}Si MAS NMR spectra of residuals after selective dissolution.

spectra, XRF and ^{29}Si MAS NMR tests were carried out to the collected residuals (unreacted fly ash). The chemical composition analysis shows that the silica (SiO_2) contents in mixes with an activator modulus of 0.8, 1.6 and 2.4 are 54.73%, 59.92% and 53.94%, respectively. Their ^{29}Si MAS NMR spectra with the deconvolution analysis are depicted in Fig. 8. It can be seen that compared to the spectrum of the original fly ash, there is a slight reduction mainly in the area representing Q4(2Al) to Q4 (4Al) groups. It is easy to understand that the peak shape of the unreacted phases is overlapped within the overall spectra. Then the silica contribution of unreacted fly ash (Si(un)%) to the overall ^{29}Si MAS NMR peak is calculated as follows (in mol.%):

$$\mathrm{Si(un)\%} = \frac{\mathrm{Si(Res)}}{\mathrm{Si(FA)+Si(Ac)}} \times 100\% \quad (2)$$

Where Si(Res) is the amount of Si from the filtered residuals, Si(FA) is the input Si from the original fly ash, and Si(Ac) is the input Si contributed by the activator.

Based on the calculation of reaction degree and XRF analysis, the value of Si(un)% can be obtained. The result shows that the contribution of unreacted silica to the total spectra is 31.6%, 44.9% and 42.4% for mixes with activator modulus of 0.8, 1.6 and 2.4, respectively. Then their peak shapes are fixed with a single factor that fits their area contributions, and subtracted from the overall NMR spectra, and by doing so the contribution of unreacted fly ash and reaction products to each Q structure can be calculated individually. The results are listed in Table 5. It can be observed that besides the unreacted phases, newly formed Q4 groups upon activation consist about 15.7–35.4% of the total reaction products. When increasing the activator modulus, more reaction products are formed in Q4 structures that with high aluminate substitutions (Q4(3-4Al)). A high activator modulus presents significantly higher contents of newly formed Q4 sites.

Table 5
Summary of the deconvolution and selective dissolution results of alkali activated fly ash.

Site type	AF-08		AF-16		AF-24	
	Un-reacted	Newly formed	Un-reacted	Newly formed	Un-reacted	Newly formed
Q4(0Al)	6.38	0.37	10.53	< 0.1	10.55	< 0.1
Q4(1Al)	12.51	2.57	15.74	5.32	14.13	6.38
Q4(2Al)	6.76	2.67	10.45	5.66	10.75	6.48
Q4(3Al)	2.49	2.94	3.63	7.82	2.89	10.30
Q4(4Al)	3.48	7.18	4.55	8.65	4.06	13.17
Q3(1Al)	–	13.56	–	16.13	–	11.09
Q2	–	9.76	–	4.28	–	1.95
Q2(1Al)	–	9.88	–	2.68	–	2.63
Q1	–	10.56	–	2.94	–	4.35
Q0	–	8.89	–	1.86	–	2.22

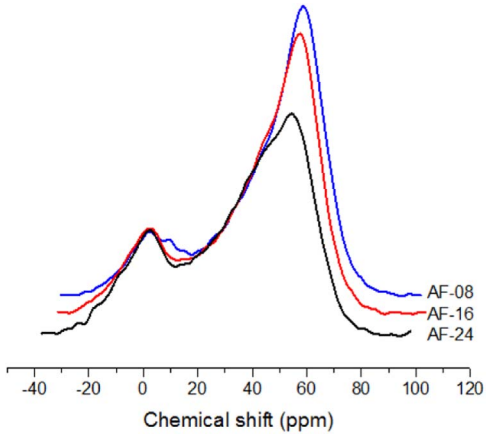

Fig. 9. The ^{27}Al MAS NMR spectra of alkali activated fly ash.

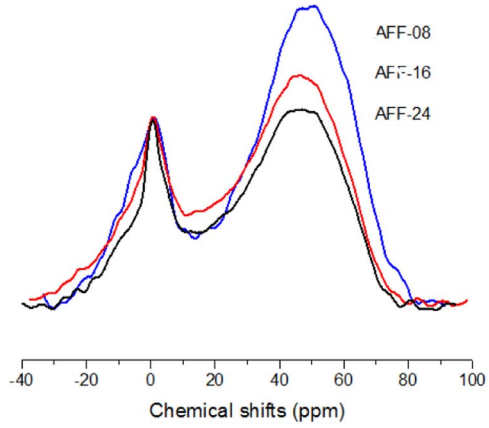

Fig. 10. The ^{27}Al MAS NMR spectra of residuals after selective dissolution.

3.3.2. ^{27}Al MAS NMR

Fig. 9 shows the ^{27}Al MAS NMR spectra of alkali activated fly ash with three different activator moduli. Two significant peaks are shown at about 2 ppm and 59–54 ppm, representing Al(IV) and Al(VI) sites within the reaction products. Also a certain amount of Al(V) contributes to the spectra since there exists a hump between around 30 and 40 ppm. Compared to the spectra of unreacted fly ash, the location of Al(VI) groups remains unchanged, indicating that the alumina contaminated crystalline phases such as mullite show limited or negligible contribution to the activation process. Besides, the relative intensity of the Al(IV) groups exhibits a significant increment, due to the massive formation within the reacted gels. The location of the Al(IV) peak in the original fly ash is at around 46 ppm, suggesting a lower silicon surrounded Al(IV) environment after activation. Compared to the spectra of alkali activated slag, due to the dramatically reduced content of reactive calcium, no hydrotalcite type phases at around 10 ppm are observed. As the activator modulus increases from 0.8 to 2.4, there is a reduction on the relative intensity of the Al(IV) groups, together with less ordered peak shape and increased intensity of Al(IV) sites. Based on the ^{29}Si MAS NMR analysis, those shifts can be partly attributed to the reduced reaction degree of fly ash, therefore more 4–6 coordinated Al groups from the original ash contribute to the overall spectrum, resulting in a lower Al(IV) to Al(IV) ratio. The obviously increased hump area around 20–40 ppm also indicates less Al(V) from the fly ash is transformed into the reaction products (tetra-Al). Meanwhile, the newly formed reaction products with mainly Al(IV) sites greatly contribute to a peak location, thus the mixtures with a higher reaction degree (lower activator modulus) present a more intensive Al(IV) peak.

The residuals of alkali activated fly ash after selective dissolution were also tested by ^{27}Al MAS NMR, and the results are shown in Fig. 10. The residuals in this case are regarded as the unreacted components of fly ash after activation. The figure shows that the residuals exhibit two significant peaks at around 1 and 46 ppm, as well as a broad hump between around 20–40 ppm, assigning to the unreacted 6, 4 and 5 coordinated Al within the unreacted phases, respectively. The unreacted Al(IV) groups are centered at around 46 ppm, presenting the same location as the original fly ash. In terms of the Al(VI) groups, the peak location is shifted from 2 to 1 ppm and exhibits an obviously sharpened size compared to the raw fly ash. The sharpened peak intensity of octa-Al can be attributed to the relatively reduced peak of tetra-Al, which is partly consumed during the alkali activation. The changed peak shape of Al(VI) groups together with the reduced peak location may suggest that the Al(VI) sites in the original fly ash are partly reacted during the alkali activation, namely the Al(VI) from glassy Al phases and/or crystalline mullite participated into the reaction process.

3.4. Alkali activated slag-fly ash blends

3.4.1. ^{29}Si MAS NMR

Fig. 11 shows the ^{29}Si MAS NMR spectra and deconvoluted peaks of alkali activated slag-fly ash blends with three different activator conditions. Similar to the spectra of alkali activated slag, the reaction products exhibit an obvious peak area between around −90 and −60 ppm, representing the large amounts of Q0 to Q2 groups within the reaction products. All peaks also show a large fraction of unreacted slag. The wide covered area at about −120 to −90 ppm is assigned to the Q4 sites, mainly from the original fly ash and its reaction products. The deconvolution results are summarized in Table 6. The mixes show similar amount of unreacted silica from the original slag around 15.8–18.8%. Also similar to the case of alkali activated slag, the fraction of Q0 and Q1 groups remains stable regardless of the activator modulus. When increasing the activator modulus from 0.8 to 2.4, the content of Q2(1Al) and Q2 groups shows a continuous reduction, up to around 8.4% and 4.4%, respectively. The fraction of Q3(1Al) groups shows a slight increase from about 7.4–11.1%, exhibiting a lower increment compared to the alkali activated slag. In terms of the Q4 content, there is an increase in general from 29.4% to 40.3% when increasing the activator modulus. This is mainly contributed by the Q4(4Al) and Q4(3Al) sites, which increase from around 12.5–22.1%; while the Q4(2Al) to Q4(0Al) group contents are less shifted, namely between approximately 16.9% and 19.1%.

The reaction degree of slag, in terms of the Si, is calculated using the same method as described in Section 3.2, while with the consideration of fly ash incorporation on the initial Si input, namely the initial silica consists of the ones from slag, fly ash and activator rather than only slag and activator. By applying the same methodology, the calculated silica reactivity from slag is 47.1%, 52.0% and 39.7% in mixes with the activator modulus of 0.8, 1.6 and 2.4, respectively. Those values are lower than the case of alkali activated slag, indicating a negative effect of fly ash incorporation on the slag reactivity. Meanwhile, similar to the measurements described in Section 3.3, the selective dissolution is carried out to the reaction products of alkali activated slag-fly ash blends, together with the XRF and ^{29}Si MAS NMR analyze of the undissolved residuals. Their ^{29}Si MAS NMR spectra with deconvolution are presented in Fig. 12, and in mixes with activator modulus of 0.8, 1.6 and 2.4, the silicate content within the residuals is 55.29%, 56.08% and 52.08%, respectively; and a dissolved fraction of 72.6%, 70.0% and 68.4%, respectively. The silica contribution of residuals to the overall ^{29}Si MAS NMR peak is calculated by (in mol.%):

$$\mathrm{Si}\% = \frac{\mathrm{Si(Res)}}{\mathrm{Si(FA)+Si(GGBS)+Si(Ac)}} \times 100\% \quad (3)$$

Where Si(Res) is the amount of Si in the residuals, Si(FA) is the amount Si from the initial fly ash, Si(GGBS) is the amount of Si from the initial

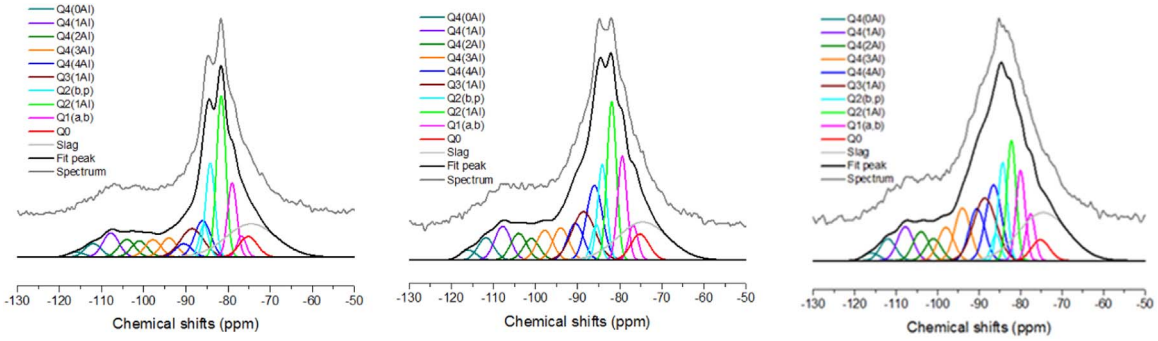

Fig. 11. The ^{29}Si MAS NMR spectra of alkali activated slag-fly ash blends.

Table 6
Deconvolution results of ^{29}Si MAS NMR spectra of alkali-activated slag- fly ash blends.

Chemical shift (± 0.5 ppm)	Site type	Sample ID		
		ASF-08	ASF-16	ASF-24
−116.0	Q4(0Al)	0.89	1.33	0.95
−112.0	Q4(0Al)	2.44	2.94	2.68
−108.0	Q4(1Al)	4.37	4.47	4.16
−104.0	Q4(2Al)	3.16	3.55	3.58
−101.0	Q4(2Al)	2.93	2.85	2.69
−98.0	Q4(3Al)	3.14	3.94	4.08
−94.0	Q4(3Al)	3.44	4.28	6.46
−91.0	Q4(4Al)	2.42	4.85	6.38
−86.0	Q4(4Al)	6.62	9.90	9.29
−88.6	Q3(1Al)	7.40	9.28	11.13
−85.5	Q2-p	3.41	2.71	1.88
−84.2	Q2-b	9.84	7.34	6.95
−81.1	Q2(1Al)	16.92	12.16	8.54
−79.3	Q1-b	7.78	7.98	6.41
−77.0	Q1-a	2.18	2.69	3.35
−75.0	Q0	4.22	3.93	2.95
−74.51	Slag	18.83	1.33	0.95

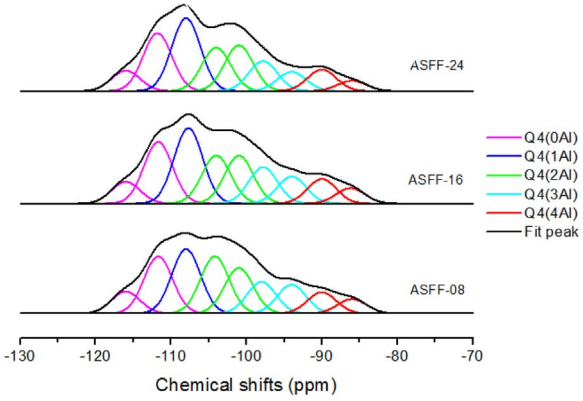

Fig. 12. The ^{29}Si MAS NMR spectra of residuals from alkali activated slag-fly ash blends.

slag, and Si(Ac) is the content of Si contributed by the activator.

The result shows that the unreacted silica contribution from the unreacted ash to the total spectra is 15.2%, 16.8% and 16.5% for mixes with activator moduli of 0.8, 1.6 and 2.4, respectively. Then the content of unreacted phases regarding each Q4 structure within the reaction products is subtracted based on their deconvolution results and peak contributions. The results are listed in Table 7. It can be seen that the Q3 to Q0 groups are newly formed low polymerized structures, while the Q4 sites include both unreacted phases and newly formed ones. Within the new phases, Q4(4Al) and Q4(3Al) exhibit an obvious increase with the increase of activator modulus, especially the Q4(4Al) groups, which occupy more than half of the newly formed

Table 7
Summary of the deconvolution and selective dissolution results of alkali activated fly ash.

Site type	ASF-08		ASF-16		ASF-24	
	Un-reacted	Newly formed	Un-reacted	Newly formed	Un-reacted	Newly formed
Q4(0Al)	3.49	< 0.1	3.91	0.36	3.98	< 0.1
Q4(1Al)	5.39	2.14	5.81	2.21	5.77	1.78
Q4(2Al)	3.43	2.64	3.96	2.83	3.90	2.88
Q4(3Al)	1.27	2.16	1.27	3.01	0.99	5.47
Q4(4Al)	1.58	7.46	1.87	12.88	1.64	14.03
Q3(1Al)	–	7.40	–	9.28	–	11.13
Q2	–	13.25	–	10.05	–	8.83
Q2(1Al)	–	16.92	–	12.16	–	8.54
Q1	–	9.96	–	10.67	–	9.76
Q0	–	4.22	–	3.93	–	2.95
Slag	18.83	–	15.81	–	18.51	–

Q4 structures. While the content of Q4 groups with 0–2 aluminate substitutions remains a similar level, showing a total fraction of about 5% within the input silicate.

3.4.2. ^{27}Al MAS NMR

The ^{27}Al MAS NMR spectra of alkali activated slag-fly ash blends with three levels of activator moduli are depicted in Fig. 13. Similar to the cases of alkali activation of sole slag or fly ash, all spectra present two typical peaks: octa-Al and tetra-Al, together with a broad hump assigned to the penta-Al. The location of Al(VI) groups is fixed at around 10 ppm, which indicates the presence of hydrotalcite type phases. Compared to alkali activated slag, this group shows the same chemical shift but with a relatively low peak intensity, revealing a relatively low content of these phases within the overall reaction products. It is easy to understand that this is due to the reduced absolute slag content in the slag-fly ash blends (slag/fly ash = 50/50).

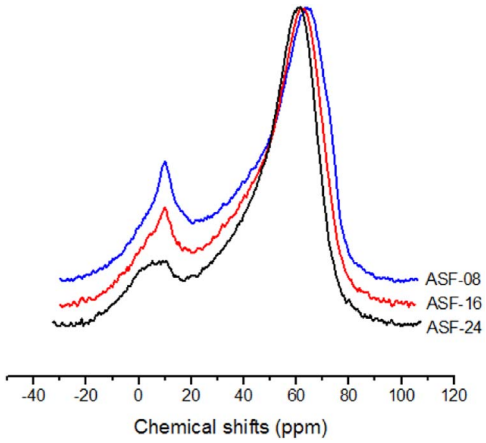

Fig. 13. The ^{27}Al MAS NMR spectra of alkali activated slag-fly ash blends.

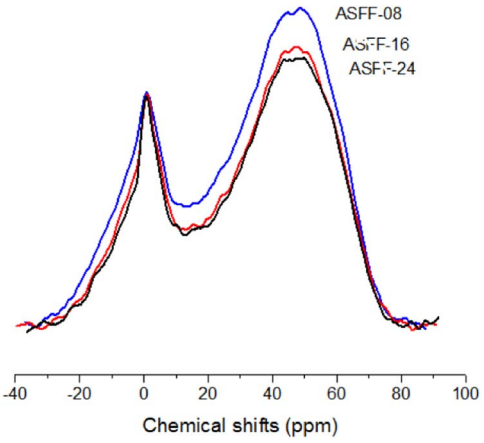

Fig. 14. The ^{27}Al MAS NMR spectra of residuals from alkali activated slag-fly ash blends.

Compared to the alkali activated fly ash, the peak of Al(VI) sites at around 2 ppm seems to be covered by the newly formed hydrotalcite typed phases and becomes no longer significant, demonstrating its relatively low content compared to the one at 10 ppm. In terms of the Al(IV) groups, the peak location is at around 63 ppm, which is similar in general as the ones observed in alkali activated slag, but higher than the case of alkali activated fly ash, showing the slight difference of Al(IV) environments between C-A-S-H and N-A-S-H type gels, also in the blended system, the Al(IV) environment tends to be similar with the low polymerized C-A-S-H type gels. When increasing the activator modulus from 0.8 to 2.4, there is an obvious reduction of relative Al(VI) content, indicating a higher transformation rate of Al(VI) to Al(IV) groups. The ^{27}Al MAS NMR spectra of insoluble residuals from alkali activated slag-fly ash blends are presented in Fig. 14. Those spectra share a very similar peak location and intensity to the residuals from the alkali activated fly ash, since they are intrinsically the same material with slightly different chemical compositions. The location of Al(VI) sites in both cases is 1 ppm, while the Al(IV) peak location shifts to 1 ppm higher than the case of alkali activated fly ash, indicating a slight difference of the activation effect on fly ash when blended alkali system is applied. Besides, a sharper peak of Al(VI) sites can be observed in mixes with higher activator modulus, which may indicate that activator solutions with a low modulus exhibit a better interaction with the Al(VI) groups, resulting in a slightly lower amount of remaining octa-Al.

3.5. Effect of activator and hybrid use of precursors on reaction degree

The chemistry, reaction kinetics, gel structure of alkali activated slag, fly ash and their blends are studied in great detail previous researches, providing strong basis for the understanding and application of this new type of binder [1,7,16–20,68]. The results in this study show similar tendency towards the previous studies regarding the effect of activator and slag-fly ash blends on the reaction process during the alkali activation. For instance, the ^{29}Si MAS NMR analysis shows that the increased activator modulus leads to a reduction on the silica reactivity, which can correspond to the decreased reaction intensity with delayed main reaction peak, as shown in the isothermal calorimetric results, also slightly reduced bond water content was reported from the TG analysis [56]. The addition of fly ash into slag leads to a more complicated chemistry, and usually presents coexisting N-A-S-H and C-(A)-S-H type gels, identified by FTIR, SEM/EDX etc. [14,15,39,69,70]; consistently, the ^{29}Si MAS NMR results in this study verify the formation of reaction products with both Q4 and chain structures. Besides the previous investigations, this study gives a special focus on analyzing the gel composition and reaction degree based on the deconvolution of ^{29}Si MAS NMR results, while the ^{27}Al MAS NMR spectra provide additional supporting information. Although the deconvolution analysis may not precisely quantify the silica structures (content and type), a consistent analyzing method applied throughout the whole study is still capable of investigating the structure shifts of alkali activated materials before and after activation. The quantified analysis provides some insights in understanding the reaction degree and reaction products, which can also be used as supplementary information of other micro scale analyses.

Fig. 15 shows a comparison of the silica structure compositions

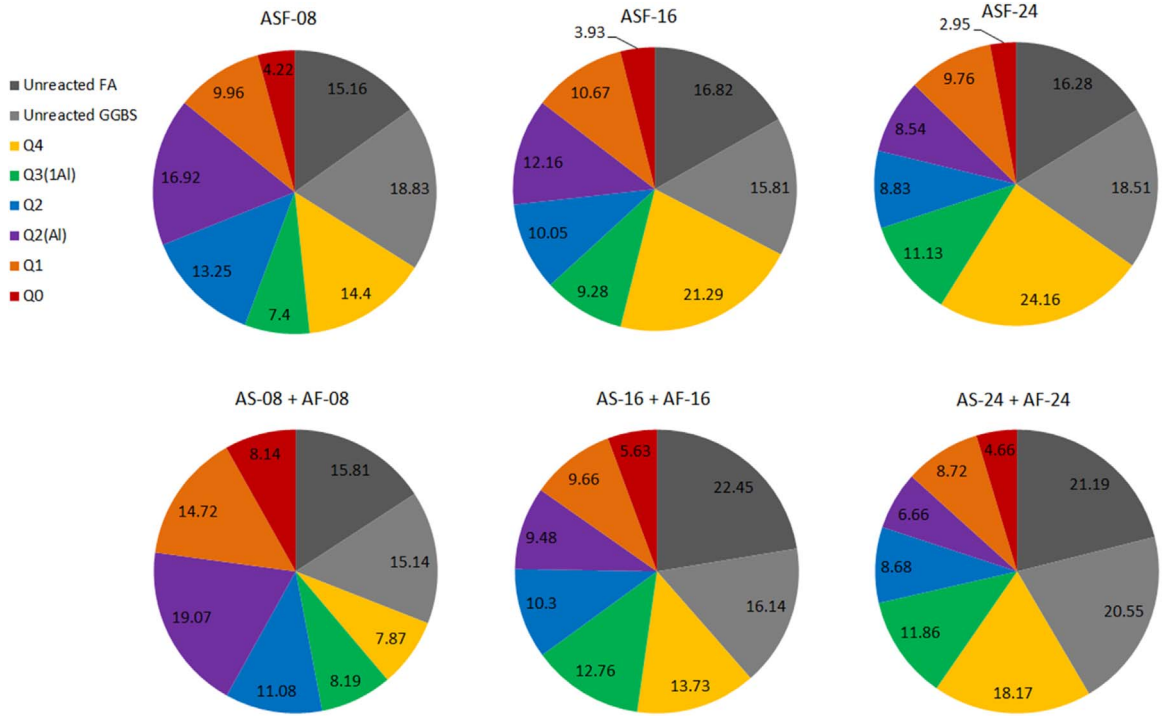

Fig. 15. Comparison of the silicate compositions.

(mol%) between alkali activated slag-fly ash blends, and a physical mix of alkali activated slag and alkali activated fly ash (50/50 by mass), the gel composition of the latter mix is obtained from the ones shown in Sections 3.1 and 3.2. It should be noticed that although the unreacted fly ash and slag content remain relatively stable as the activator modulus increases, there is still a significant difference in reactivity of the raw materials, due to the shifted additional silicate content from the activators. The silicate from the activator presents a considerable amount of the total silica input, which is about 3.87, 7.72 and 11.58 g per 100 g of the precursors. Comparing the reactivity results in Sections 3.2–3.4, it is shown that when blended system is applied, there is a slight reduction of the slag reactivity and an increase of the reaction degree of fly ash, confirming an interaction between the precursors. The alkali activated slag-fly ash blends and the hypothesized AA-slag + AA-fly ash mixes are having the same starting compositions, the different silicate compositions in the reaction products also suggest an interaction. For mixes with an activator modulus of 0.8, the content of unreacted silica contains around 34.0% of the total silica, namely about 66.0% of the input silica is participated into the reaction products; while it should be noted that all the silicate from the initial activator (about 8% in sample ASF-08) is also considered as reaction products in this case, since it is impossible to distinguish their silicate origins from the reaction products. Compared to the AS-08 + AF-08 mix, the content of Q0 and Q1 groups is reduced by 3.9% and 4.8%, respectively; while the Q4 groups show an increment of around 6.5% (mainly contributed by Q4(4Al)). The reduced content of isolated silicate, end-of-chain structures together with the increased Q4 sites suggest a higher polymerization and crosslinking in the blended system. Besides, the content of Q3 and Q2 groups remains similar, with slightly reduced Q2(1Al) content of around 2.2%, increased Q2 content of 2.2% and Q3(1Al) shifts less than 1%. As the activator modulus increases to 1.6 and 2.4, the silicate from activator occupies 14.8% and 20.6% of the total silicate input. Thus although similar contents of unreacted slag and fly ash are presented, differences in reactivity are still shown by using the methodology described in Sections 3.1–3.4. Compared to the physically mixed samples with a fixed activator modulus, there is a reduction on the unreacted starting materials, indicating that the blended system benefits the overall reaction degree; with largely increased content of Q4 structures, increased Q2(1Al) sites, slightly reduced Q3(1Al) and Q0 groups, and similar Q1 and Q2 contents.

Based on the deconvolution results of ^{29}Si MAS NMR rspectra, the average chain length and Si/Al in the reaction products are calculated and listed in Table 8. The mean chain length (MCL), Si/Al of C-A-S-H and N-A-S-H type gels are calculated by :

$$MCL = \frac{Q1+\frac{3}{2}Q2(1Al)+Q2}{\frac{1}{2}Q1} \quad (4)$$

$$Si/Al_{CASH} = \frac{Q1 + Q2 + Q2(1Al)}{\frac{1}{2}Q2(1Al)} \quad (5)$$

Table 8
Calculation of mean chain length and Si/Al of the reaction products.

Sample ID	Si/Al in C-A-S-H	MCL	Si/Al in N-A-S-H
AS-08	4.21	7.80	–
AS-16	6.02	6.97	–
AS-24	7.33	6.80	–
AF-08	–	–	1.38
AF-16	–	–	1.47
AF-24	–	–	1.41
ASF-08	4.74	9.76	1.32
ASF-16	5.41	7.30	1.24
ASF-24	6.35	6.43	1.20

$$Si/Al_{NASH} = \frac{\sum_{n=0}^{4} Q4(nAl)}{\sum_{n=0}^{4} \frac{n}{4}Q4(nAl)} \quad (6)$$

It can be seen that as the activator modulus increases, the mean chain length of the formed C-A-S-H type gels is slightly reduced with an obviously increased Si/Al. In the case of alkali activated fly ash, it should be noticed that only the newly formed Q4 structures are applied in the calculation, the Si/Al in the N-A-S-H is relatively stable regardless of the activator modulus: between 1.38 and 1.47. When blended precursor is applied, mixes with an activator modulus of 0.8 exhibits a slight increase in Si/Al in terms of the C-A-S-H type gels, while the other two show a reduction. The mean chain length presents an increase in general except the mix with a modulus of 2.4. Concerning the Si/Al in the N-A-S-H type gels, there is a reduction as the activator modulus increases, compared to the alkali activated purely fly ash. All those shift confirm again the gel interaction in the blended binder system.

4. Conclusions

This paper investigates the effect of activator modulus on the reaction degree of alkali activated slag, fly ash and slag-fly ash composites. The reaction degree is identified by applying selective dissolution and ^{29}Si MAS NMR spectra deconvolutions. ^{27}Al MAS NMR also applied as a supplement to understand the gel structure. The combined application of these two methods brings a new approach in identifying the reactivity of the starting materials and characterizing the reaction products, which provides further insights in understanding the microstructure and stoichiometry of alkali activated slag, fly ash and their blends. The following conclusions can be drawn based on the results:

- For alkali activated slag, increasing the activator modulus reduces the slag reactivity by about 66–45%, with the reduced content of Q2(1Al) groups and increased content of Q3(1Al) sites. Hydrotalcite type phases are observed, and increasing activator modulus reduces the relative content of Al(VI) within the reaction products.
- The unreacted fly ash and reaction products are separated by selective dissolution, which were then analyzed by ^{29}Si, ^{27}Al MAS NMR, and XRF. Increase the activator modulus results in an increased content of Q4 groups, while reduced reaction degree of fly ash. Both polymerized Q4 structures and short ranged Q2 to Q0 sites are formed. The contribution of unreacted ash and reaction products to a certain silica structure are identified. Octa-Al located at around 2 ppm remains in the reaction products, while a more intense Al(VI) peak at 1 ppm is observed within the undissolved phases.
- In the blended binder system, the slag reactivity is reduced while the reaction degree of fly ash is increased. Both C-A-S-H and N-A-S-H type gels are identified within the reaction products. The Q4(4Al) groups consist more than half of the newly formed Q4 structures.
- Compared to the mixture of alkali activated slag and alkali activated fly ash with the same chemical composition, the blended binder exhibits higher contents of newly formed Q4 groups with reduced Si to Al ratios, and reduced content of Q0 groups, shifted mean chain length and Si/Al of the C-A-S-H type gels, showing a gel interaction when blended binders is applied.

Acknowledgements

This research was supported by China Scholarship Council (201306950046) and the Department of the Built Environment at Eindhoven University of Technology. The authors thank Prof.dr. F.Z. Wang and Prof.dr. W. Chen from the State Key Laboratory of Silicate Materials for Architectures, Wuhan University of Technology, PR

China, for the use of NMR instrument. Further the authors wish to express their gratitude to the following sponsors of the Building Materials Research Group at TU Eindhoven: Rijkswaterstaat Grote Projecten en Onderhoud; Graniet-Import Benelux; Kijlstra Betonmortel; Struyk Verwo; Attero; Enci; Rijkswaterstaat Zee en Delta-District Noord; Van Gansewinkel Minerals; BTE; V.d. Bosch Beton; Selor; GMB; Geochem Research; Icopal; BN International; Eltomation; Knauf Gips; Hess AAC Systems; Kronos; Joma; CRH Europe Sustainable Concrete Centre; Cement & Beton Centrum; Heros and Inashco (in chronological order of joining).

References

[1] M. Shojaei, K. Behafarnia, R. Mohebi, Application of alkali-activated slag concrete in railway sleepers, Mater. Des. 69 (2015) 89–95.
[2] A.M. Rashad, A comprehensive overview about the influence of different admixtures and additives on the properties of alkali-activated fly ash, Mater. Des. 53 (2014) 1005–1025.
[3] S.D. Wang, K.L. Scrivener, P.L. Pratt, Factors affecting the strength of alkali-activated slag, Cem. Concr. Res. 24 (6) (1994) 1033–1043.
[4] S. Aydin, B. Baradan, Mechanical and microstructural properties of heat cured alkali-activated slag mortars, Mater. Des. 35 (2012) 374–383.
[5] Y.Z. Hai, Venkatesh Kodur, L.Q. Shu, C. Liang, W. Bo, Development of metakaolin-fly ash based geopolymers for fire resistance applications, Constr. Build. Mater. 55 (2014) 38–45.
[6] W. Zhou, et al., A comparative study of high- and low-Al2O3 fly ash based-geopolymers: the role of mix proportion factors and curing temperature, Mater. Des. 95 (2016) 63–74.
[7] Li Chao, Sun Henghu, Li Longtu, A review: the comparison between alkali-activated slag (Si+Ca) and metakaolin (Si+Al) cements, Cem. Concr. Res. 40 (2010) 1341–1349.
[8] A.R. Brough, A. Atkinson, Sodium silicate-based alkali-activated slag mortars: part I. Strength, hydration and microstructure, Cem. Concr. Res. 32 (2002) 865–879.
[9] M.L. Granizo, S. Alonso, M.T. Blanco-Varela, A. Palomo, Alkaline activation of metakaolin: effect of calcium hydroxide in the products of reaction, J. Am. Ceram. Soc. 85 (1) (2002) 225–231.
[10] M. Rashad Alaa, Properties of alkali-activated fly ash concrete blended with slag, Iran. J. Mater. Sci. Eng. 10 (1) (2013) 57–64.
[11] S. Aydin, A ternary optimization of mineral additives of alkali activated cement mortars, Constr. Build. Mater. 43 (2013) 131–138.
[12] T. Sugama, L.E. Brothers, T.R. Van de Putte, Acid-resistant cements for geothermal wells: sodium silicate activated slag/fly ash blends, Adv. Cem. Res. 17 (2) (2005) 65–75.
[13] N.K. Lee, H.K. Lee, Setting and mechanical properties of alkali-activated fly ash/slag concrete manufactured at room temperature, Constr. Build. Mater. 47 (2013) 1201–1209.
[14] I. García-Lodeiro, D.E. Macphee, A. Palomo, A. Fernández-Jiménez, Effect on fresh C-S-H gels the simultaneous addition of alkali and aluminium, Cem. Concr. Res. 40 (2010) 27–32.
[15] I. Ismail, S.A. Bernal, J.L. Provis, R.S. Nicolas, S. Hamdan, J.S.J. Deventer, Modification of phase evolution in alkali-activated blast furnace slag by the incorporation of fly ash, Cem. Concr. Compos. 45 (2014) 125–135.
[16] C.K. Yip, G.C. Lukey, J.S.J. van Deventer, The coexistence of geopolymeric gel and calcium silicate hydrate at the early stage of alkaline activation, Cem. Concr. Res. 35 (2005) 1688–1697.
[17] I. García-Lodeiro, A. Fernández-Jiménez, A. Palomo, D.E. Macphee, Effect of calcium additions on N-A-S-H cementitious gels, J. Am. Ceram. Soc. (2010) 1–7.
[18] I. García-Lodeiro, A. Fernández-Jiménez, M.T. Blanco, A. Palomo, FTIR study of the sol-gel synthesis of cementitious gels: C-S-H and N-A-S-H, J. Sol-Gel Sci. Technol. 45 (2008) 63–72.
[19] I. García-Lodeiro, D.E. Macphee, A. Palomo, A. Fernández-Jiménez, Effect of alkalis on fresh C-S-H gels. FTIR analysis, Cem. Concr. Res. 39 (2009) 147–153.
[20] B.A. Bernal, J.L. Provis, B. Walkerly, et al., Gel nanostructure in alkali-activated binders based on slag and fly ash, and effects of accelerated carbonation, Cem. Concr. Res. 53 (2013) 127–144.
[21] G.K. Sun, J.F. Young, R.J. Kirkpatrick, The role of Al in C-S-H: NMR, XRD, and compositional results for precipitated samples, Cem. Concr. Res. 36 (1) (2006) 18–29.
[22] P.J. Schilling, L.G. Butler, A. Roy, H.C. Eaton, ^{29}Si and ^{27}Al MAS NMR of NaOH-activated blast-furnace slag, J. Am. Ceram. Soc. 77 (9) (1994) 2363–2368.
[23] F. Bonk, J. Schneider, M.A. Cincotto, H. Panepucci, Characterization by multi-nuclear high-resolution NMR of hydration products in activated blast-furnace slag pastes, J. Am. Ceram. Soc. 86 (10) (2003) 1712–1719.
[24] S.D. Wang, K.L. Scrivener, Hydration products of alkali-activated slag cement, Cem. Concr. Res. 25 (3) (1995) 561–571.
[25] S.D. Wang, K.L. Scrivener, ^{29}Si and ^{27}Al NMR study of alkali-activated slag, Cem. Concr. Res. 33 (5) (2003) 769–774.
[26] P. Rejmak, J.S. Dolado, M.J. Stott, A. Ayudala, ^{29}Si NMR in cement: a theoretical study on calcium silicate hydrates, J. Phys. Chem. C 116 (2012) 9755–9761.
[27] A. Fernandez, F. Puertas, I. Sobrados, J. Sanz, Structure of calcium silicate hydrates formed in alkaline-activated slag: influence of the type of alkaline activator, J. Am. Ceram. Soc. 86 (8) (2003) 1389–1394.
[28] M. Palacios, F. Puertas, Effect of carbonation on alkali-activated slag paste, J. Am. Ceram. Soc. 89 (10) (2006) 3211–3221.
[29] T. Hakkinen, The influence of slag content on the microstructure, permeability and mechanical properties of concrete: Part 1. Microstructural studies and basic mechanical properties, Cem. Concr. Res. 23 (2) (1993) 407–421.
[30] S.M. Park, J.G. Jang, N.K. Lee, H.K. Lee, Physicochemical properties of binder gel in alkali-activated fly ash/slag exposed to high temperatures, Cem. Concr. Res. 89 (2016) 72–79.
[31] Z.H. Peng, K. Vance, A. Dakhane, R. Marzke, N. Neithalath, Microstructural and ^{29}Si MAS NMR spectroscopic evaluations of alkali cationic effects on fly ash activation, Cem. Concr. Compos. 57 (2015) 34–43.
[32] A. Fernandez, A.G. Torre, A. Palomo, G. Lopez, M.M. Alonso, M.A.G. Aranda, Quantitative determination of phases in the alkali activation of fly ash. Part I. Potential ash reactivity, Fuel 85 (2006) 625–634.
[33] M. Criado, A. Fernandez, A. Palomo, I. Sobrados, J. Sanz, Effect of the SiO2/Na2O ratio on the alkali activation of fly ash. Part II: 29Si MAS NMR survey, Micro Meso Mater. 109 (2008) 525–534.
[34] A. Fernandez, A.G. Torre, A. Palomo, G. Lopez, M.M. Alonso, M.A.G. Aranda, Quantitative determination of phases in the alkaline activation of fly ash. Part II: degree of reaction, Fuel 85 (2006) 1960–1969.
[35] G. Kovalchuk, A. Fernandez, A. Palomo, Alkali-activated fly ash: effect of thermal curing conditions on mechanical and microstructural development – Part II, Fuel 86 (2007) 315–322.
[36] G. Saout, H.M. Ben, F. Winnefeld, B. Lothenbach, Hydration degree of alkali-activated slags: a ^{29}Si NMR study, J. Am. Ceram. Soc. 94 (12) (2011) 4541–4547.
[37] B. Walkley, et al., Phase evolution of C-(N)-A-S-H/N-A-S-H gel blends investigated via alkali-activation of synthetic calcium aluminosilicate precursors, Cem. Concr. Res. 89 (2016) 120–135.
[38] B. Walkley, et al., Synthesis of stoichiometrically controlled reactive aluminosilicate and calcium-aluminosilicate powders, Powder Technol. 297 (2016) 17–33.
[39] N.K. Lee, H.K. Lee, Reactivity and reaction products of alkali-activated, fly ash/slag paste, Constr. Build. Mater. 81 (2015) 303–312.
[40] J.E. Oh, Y.B. Jun, Y. Jeong, Characterization of geopolymers from compositionally and physically different Class F fly ashes, Cem. Concr. Compos. 50 (2014) 16–26.
[41] X.L. Pardal, F. Brunet, T. Charpentier, I. Pochard, A. Nonat, ^{27}Al and ^{29}Si solid-state NMR characterization of calcium-aluminosilicate-hydrate, Inorg. Chem. 51 (2012) 1827–1836.
[42] F. Puertas, M. Palaciosc, H. Manzanod, J.S. Doladod, A. Ricof, J. Rodríguezf, A model for the C-A-S-H gel formed in alkali-activated slag cements, J. Eur. Ceram. Soc. 31 (2011) 2043–2056.
[43] E. Lhopital, B. Lothenbach, G. Saout, D. Kulik, K.L. Scrivener, Incorporation of aluminium in calcium-silicate-hydrates, Cem. Concr. Res. 75 (2015) 91–103.
[44] I. Garcia, A. Fernandez, A. Palomo, Variation in hybrid cements over time. Alkaline activation of fly ash–portland cement blends, Cem. Concr. Res. 52 (2013) 112–122.
[45] F. Puertas, A. Fernandez, Mineralogical and microstructural characterization of alkali-activated fly ash/slag pastes, Cem. Concr. Compos. 25 (2003) 287–292.
[46] A. Buchwald, H. Hilbig, C. Kaps, Alkali-activated metakaolin-slag blends, performance and structure in dependence of their composition, J. Mater. Sci. 42 (2007) 3024–3032.
[47] S. Puligilla, P. Mondal, Co-existence of aluminosilicate and calcium silicate gel characterized through selective dissolution and FTIR spectral subtraction, Cem. Concr. Res. 70 (2015) 39–49.
[48] A. Fernandez, A. Palomo, Mid-infrared spectroscopic studies of alkali activated fly ash structure, Micro Meso Mater. 86 (1) (2005) 207–214.
[49] A. Palomo, S. Alonso, A. Fernandez, I. Sobrados, J. Sanz, Alkaline activation of fly ashes: nmr study of the reaction products, J. Am. Ceram. Soc. 87 (2004) 1141–1145.
[50] A. Fernandez, A. Palomo, Characterisation of fly ashes. Potential reactivity as alkaline cements, Fuel 82 (2003) 2259–2265.
[51] L.H. Merwin, A. Sebald, H. Rager, H. Schneider, ^{29}Si and ^{27}Al MAS NMR spectroscopy of mullite, Phys. Chem. Miner. 18 (2003) 47–52.
[52] S.A. Bernal, et al., MgO content of slag controls phase evolution and structural changes induced by accelerated carbonation in alkali-activated binders, Cem. Concr. Res. 57 (2014) 33–43.
[53] R.J. Myers, S.A. Bernal, R.S. Nicolas, J.L. Provis, Generalized structural description of calcium-sodium aluminosilicate hydrate gels: the cross-linked substituted tobermorite model, Langmuir 29 (2013) 5294–5306.
[54] X.L. Pardal, F. Brunet, T. Charpentier, I. Pochard, A. Nonat, ^{27}Al and ^{29}Si solid-state NMR characterization of calcium-aluminosilicate-hydrate, Inorg. Chem. 51 (2012) 1827–1836.
[55] I.G. Richardson, The calcium silicate hydrates, Cem. Concr. Res. 38 (2008) 137–158.
[56] X. Gao, Q.L. Yu, H.J.H. Brouwers, Reaction kinetics, gel character and strength of ambient temperature cured alkali activated slag-fly ash blends, Constr. Build. Mater. 80 (2015) 105–115.
[57] X. Gao, Q.L. Yu, H.J.H. Brouwers, Properties of alkali activated slag-fly ash blends with limestone addition, Cem. Concr. Compos. 59 (2015) 119–128.
[58] X. Gao, Q.L. Yu, H.J.H. Brouwers, Assessing the porosity and shrinkage of alkali activated slag-fly ash composites designed applying a packing model, Constr. Build. Mater. 119 (2016) 175–184.
[59] H. Jansson, D. Bernin, K. Ramser, Silicate species of water glass and insights for alkali-activated green cement, AIP Adv. 5 (067167) (2015) 1–9.
[60] P. Faucon, A. Delagrave, J.C. Petit, C. Richet, J.M. Marchand, H. Zanni, Aluminum incorporation in calcium silicate hydrates (C-S-H) depending on their Ca/Si ratio, J. Phys. Chem. B 103 (37) (1999) 7796–7802.
[61] G.L. Saout, M.B. Haha, F. Winnefeld, B. Lothenbach, Hydration degree of alkali-

activated slags: a ^{29}Si NMR study, J. Am. Ceram. Soc. 94 (2011) 4541–4547.
[62] K.J.D. MacKenzie, R.H. Meinhold, B.L. Sherriff, Z. Xu, ^{27}Al and ^{25}Mg solid-state magic-angle spinning nuclear magnetic resonance study of hydrotalcite and its thermal decomposition sequence, J. Mater. Chem. 3 (12) (1993) 1263–1269.
[63] P.J. Schilling, L.G. Butler, A. Roy, A.H. Eaton, ^{29}Si and ^{27}Al MAS NMR of NaOH activated blast-furnace slag, J. Am. Ceram. Soc. 77 (9) (1994) 2363–2368.
[64] X.L. Pardal, I. Pochard, A. Nonat, Experimental study of Si–Al substitution in calcium-silicate-hydrate (C-S-H) prepared under equilibrium conditions, Cem. Concr. Res. 39 (2009) 637–643.
[65] M.H. Ben, G.L. Saout, F. Winnefeld, B. Lothenbach, Influence of activator type on hydration kinetics, hydrate assemblage and microstructural development of alkali activated blast-furnace slags, Cem. Concr. Res. 41 (2011) 301–310.
[66] J.G.S. Jaarsveld, J.S.J. Devnter, G.C. Lukey, The effect of composition and temperature on the properties of fly ash- and kaolinite-based geopolymers, J. Chem. Eng. 89 (2002) 63–73.
[67] Engelhardt G, Michel D. High-resolution Solid-state NMR of Silicates and Zeolites, 1987.
[68] S. Kumar, R. Kumar, S.P. Mehrotra, Influence of granulated blast furnace slag on the reaction, structure and properties of fly ash based geopolymer, J. Mater. Sci. 45 (3) (2010) 607–615.
[69] D. Elisabeth, S.G. Berhan, P. Sulapha, Influence of starting material on the early age hydration kinetics, microstructure and composition of binding gel in alkali activated binder systems, Cem. Concr. Compos. 48 (2014) 108–117.
[70] I. Garcia-Lodeirov, A. Palomo, A. Fernandez, D.E. Macphee, Compatibility studies between N-A-S-H and C-A-S-H gels. Study in the ternary diagram Na_2O-CaO-Al_2O_3-SiO_2-H_2O, Cem. Concr. Res. 41 (2011) 923–931.